JACS
JOURNAL OF THE AMERICAN CHEMICAL SOCIETY
Article
pubs.acs.org/JACS

An Activity-Based Near-Infrared Glucuronide Trapping Probe for Imaging β-Glucuronidase Expression in Deep Tissues

Ta-Chun Cheng,[†,◆] Steve R. Roffler,[‡,◆] Shey-Cherng Tzou,[§] Kuo-Hsiang Chuang,[§] Yu-Cheng Su,[‡,∥] Chih-Hung Chuang,[⊥] Chien-Han Kao,[†] Chien-Shu Chen,[#] I-Hong Harn,[§] Kuan-Yi Liu,[○] Tian-Lu Cheng,*[,§,▽] and Yu-Ling Leu*[,○]

[†]Graduate Institute of Medicine, Kaohsiung Medical University, Kaohsiung, Taiwan
[‡]Institute of Biomedical Sciences, Academia Sinica, Taipei, Taiwan
[§]Department of Biomedical Science and Environmental Biology, Kaohsiung Medical University, Kaohsiung, Taiwan
[∥]Institute of Microbiology and Immunology, National Yang-Ming University, Taipei, Taiwan
[⊥]Institutes of Basic Medical Sciences, National Cheng Kung University, Tainan, Taiwan
[#]School of Pharmacy, China Medical University, Taichung, Taiwan
[▽]Cancer Center, Kaohsiung Medical University Hospital, Kaohsiung, Taiwan
[○]Department of Pharmacy, Chia Nan University of Pharmacy and Science, Tainan, Taiwan

Supporting Information

ABSTRACT: β-glucuronidase is an attractive reporter and prodrug-converting enzyme. The development of near-IR (NIR) probes for imaging of β-glucuronidase activity would be ideal to allow estimation of reporter expression and for personalized glucuronide prodrug cancer therapy in preclinical studies. However, NIR glucuronide probes are not yet available. In this work, we developed two fluorescent probes for detection of β-glucuronidase activity, one for the NIR range (containing IR-820 dye) and the other for the visible range [containing fluorescein isothiocyanate (FITC)], by utilizing a difluoromethylphenol−glucuronide moiety (TrapG) to trap the fluorochromes in the vicinity of the active enzyme. β-glucuronidase-mediated hydrolysis of the glucuronyl bond of TrapG generates a highly reactive alkylating group that facilitates the attachment of the fluorochrome to nucleophilic moieties located near β-glucuronidase-expressing sites. FITC-TrapG was selectively trapped on purified β-glucuronidase or β-glucuronidase-expressing CT26 cells (CT26/mβG) but not on bovine serum albumin or non-β-glucuronidase-expressing CT26 cells used as controls. β-glucuronidase-activated FITC-TrapG did not interfere with β-glucuronidase activity and could label bystander proteins near β-glucuronidase. Both FITC-TrapG and NIR-TrapG specifically imaged subcutaneous CT26/mβG tumors, but only NIR-TrapG could image CT26/mβG tumors transplanted deep in the liver. Thus NIR-TrapG may provide a valuable tool for visualizing β-glucuronidase activity in vivo.

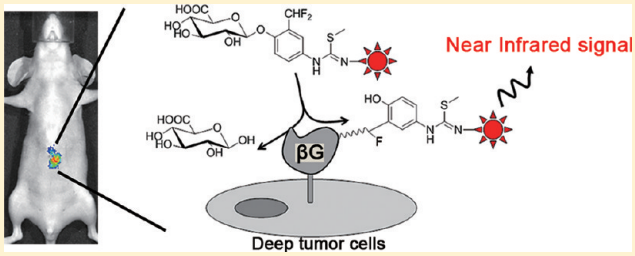

INTRODUCTION

β-glucuronidase (βG) is a lysosomal enzyme[1,2] that has been used as a tumor marker,[2−4] a prodrug-converting enzyme for cancer prodrug therapies,[5,6] and a reporter gene for tracking the location of gene delivery vectors in preclinical studies.[7−10] The ability to image βG activity in vivo would greatly improve βG-based applications. However, most βG probes are suitable only for in vitro studies and are not yet available for in vivo imaging of βG activity. For example, naphthol AS-BI β-D-glucuronide,[11,12] *p*-nitrophenyl-β-D-glucuronide (*p*-NPG),[13] and 5-bromo-4-chloro-3-indolyl-β-D-glucuronic acid (X-GlcA, X-Gluc)[14,15] are commonly used to detect βG activity in cultured cells and histological sections, but these colorimetric substrates have poor sensitivities and relatively narrow dynamic ranges and hence are not useful in vivo. In an attempt to overcome this problem, a range of fluorogenic substrates, such as fluorescein di-β-D-glucuronide (FDGlcU)[9] and 4-methylumbelliferyl β-D-glucuronide (MU-GlcA)[14] have been developed to increase the detection sensitivity. Our previous study demonstrated that FDGlcU can be used to determine βG activity both in vitro and in vivo.[9] The penetrability of FDGlcU, however, is insufficient to image βG-expressing tumors in deep organs in living animals. Moreover, the signal generated with the FDGlcU probe rapidly diffuses away from βG-expressing sites and therefore only allows imaging of subcutaneous βG-expressing tumors over a relatively narrow time window.[9] Thus, the development of an activity-based near-IR (NIR) fluorescent glucuronide probe (λ_{em} > 800 nm) may facilitate imaging of deep tissues and improve the imaging resolution for βG.

Received: October 4, 2011
Published: January 12, 2012

   dx.doi.org/10.1021/ja209335z | J. Am. Chem. Soc. 2012, 134, 3103−3110

In this study, we developed NIR-TrapG, an activity-based NIR-fluorescent difluoromethylphenol−glucuronide probe. βG-mediated hydrolysis of the glucuronyl bond generates a highly reactive quinine methide intermediate that facilitates the attachment of the fluorochrome to nucleophilic side chains near βG-expressing sites (Figure 1). The NIR-TrapG probe is

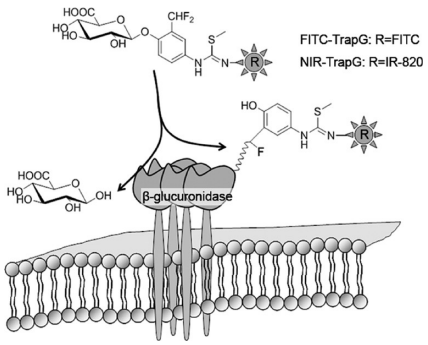

Figure 1. Mechanism of the βG activity-based trapping probe. βG-mediated hydrolysis of the glucuronyl bond generates a highly reactive quinine methide intermediate that leads to cross-linking of the probe to nearby nucleophiles.

advantageous in that it provides a specific and direct "activity-based" enzyme profile for βG. In addition, the high penetrability of NIR signals could make this strategy useful for deep-tissue imaging.[16−18] Furthermore, activity-based probes have been developed for in vivo profiling of enzymatic activities.[19−22]

Here we report the design and synthesis of two fluorescent probes for βG: NIR-TrapG and FITC-TrapG. We first examined the specificity of these trapping probes by incubating FITC-TrapG with recombinant *Escherichia coli* βG (eβG) or βG-expressing mouse colon cancer cells (CT26/mβG) in vitro. We investigated whether alkylation by activated FITC-TrapG affects the βG activity and whether FITC-TrapG could label bystander proteins in the vicinity of βG activity. Finally, we examined whether NIR-TrapG or FITC-TrapG could specifically image the location of βG-expressing CT26 tumors transplanted under the skin or deep in the livers of mice. NIR-TrapG displayed high tissue penetrability and thus may be a useful tool for tracking βG activity in vivo and for optimizing preclinical βG-based therapies and imaging systems.

RESULTS

Development of Glucuronide Trapping Probes. To develop novel glucuronide trapping probes, fluorescein isothiocyanate (FITC) and the dye IR-820 were linked to a glucuronide group via a difluoromethylphenol trapping moiety to form FITC-TrapG and NIR-TrapG, respectively. The glucuronide group acts as a hydrophilic and cell-impermeable βG substrate. βG-mediated hydrolysis of the glucuronyl bond in the probe exposes the quinine methide group, which can cross-link FITC or IR-820 to nearby nucleophiles (Figure 1). The design and synthesis of FITC-TrapG and NIR-TrapG are shown in Schemes 1−5 (see the Experimental Section). Details of the syntheses are described in the Experimental Section and the Supporting Information.

Characterization of Glucuronide Trapping Probes in Vitro. To examine whether βG can specifically activate FITC-TrapG and expose the reactive alkylating group in vitro, increasing amounts of FITC-TrapG were incubated with either purified eβG or bovine serum albumin (BSA) adsorbed in

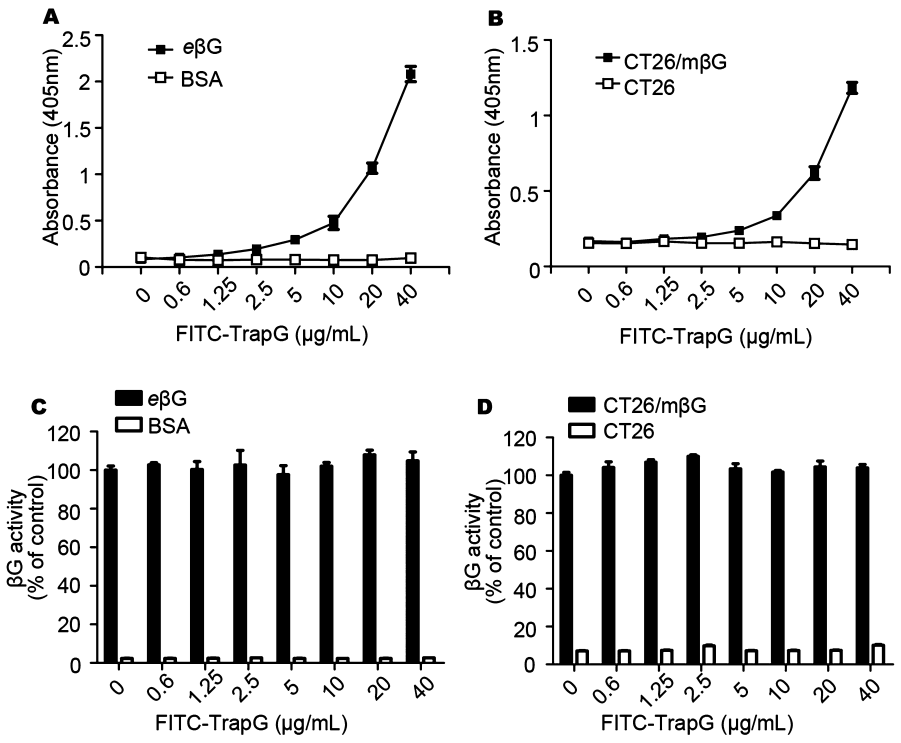

Figure 2. βG-specific activation of FITC-TrapG in vitro. Increasing amounts of FITC-TrapG were incubated with (A) βG (■) or BSA (□) or (B) CT26/mβG (■) or CT26 (□) precoated on the wells of a microtiter plate. Activation and trapping of FITC-TrapG was determined by ELISA using an anti-FITC antibody. After FITC-TrapG treatment, the βG activity was determined by hydrolysis of the *p*-NPG substrate in (C) purified proteins (eβG, BSA) or (D) cells (CT26/mβG, CT26).

dx.doi.org/10.1021/ja209335z | *J. Am. Chem. Soc.* 2012, 134, 3103−3110

microtiter plates. After excess probe was washed away, FITC attached to proteins in the wells was detected by enzyme-linked immunosorbent assay (ELISA) using an anti-FITC antibody. Figure 2A shows that the absorbance at 405 nm increased with increasing concentrations of the probe added to eβG. Conversely, incubation of FITC-TrapG with BSA did not result in accumulation of FITC in the wells. Similarly, mouse βG (mβG) expressed on the surface of CT26 cells activated FITC-TrapG and showed trapping of FITC (Figure 2B). No color development was noted after the addition of FITC-TrapG to parental CT26 cells. These results indicate that the glucuronide trapping probes were specifically activated by βG and stably retained. Furthermore, activated FITC-TrapG did not hamper βG activity, as 100% enzymatic activity was maintained even at the highest concentration of FITC-TrapG (40 μg/mL) (Figure 2C,D). We conclude that activated FITC-TrapG can be retained at sites of βG activity without affecting its enzymatic activity.

Conceptually, the activated FITC-TrapG probe can alkylate any nucleophile in close proximity to βG. To test whether the activated probes could label bystander nucleophiles, we added FITC-TrapG to a mixture of eβG and BSA in solution. Addition of FITC-TrapG resulted in labeling of FITC groups on both eβG (74 kDa) and BSA (66 kDa) (Figure 3). In the absence of βG-mediated activation, FITC-TrapG did not label the control protein BSA. We conclude that activated FITC-TrapG can label bystander nucleophiles in the vicinity of βG enzyme activity.

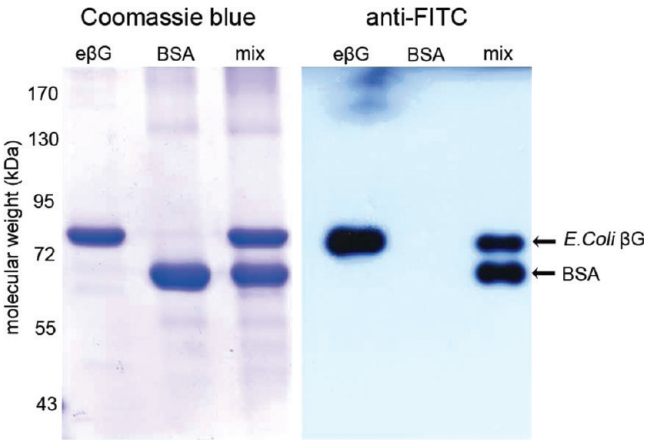

Figure 3. Bystander trapping by FITC-TrapG. FITC-TrapG was incubated with eβG, BSA, or a mixture of eβG and BSA. Activation and trapping of FITC-TrapG on proteins was detected by western blotting using an anti-FITC antibody (right panel). Protein loading was visualized by Coomassie blue staining (left panel).

Imaging of βG Activity in Subcutaneous Tumors. To examine whether the glucuronide trapping probes can specifically detect βG activity in vivo, we intravenously injected FITC-TrapG into BALB/c nude mice bearing subcutaneous CT26 or CT26/mβG tumors. Fluorescent signals were measured in live mice with a noninvasive optical imaging system. Figure 4A shows that the fluorescence intensity (defined as photons s^{-1} cm^{-2} sr^{-1}) in the CT26/mβG tumors was 4.59, 3.86, and 2.86 times greater than that in the control CT26 tumors at 24, 48, and 72 h, respectively. In line with the imaging results, FITC-derived fluorescence was retained in CT26/mβG tumors but not the control CT26 tumors, which was consistent with X-GlcA staining for βG activity (Figure 4B). Similarly, NIR-TrapG could specifically label βG-expressing cells in vitro and subcutaneous βG-expressing tumors in vivo (Figure 5). The cell-associated NIR intensity was 2.4, 2.6, and 2.8 times greater in CT26/mβG cells than in the control CT26 cells upon pretreatment with 0.5, 1, and 2 μg/mL NIR-TrapG, respectively (Figure 5A). The NIR fluorescence signal was 4.25, 4.92, and 5.21 times greater in subcutaneous CT26/mβG tumors than in the control CT26 tumors at 24, 48, and 72 h, respectively, after probe injection (Figure 5B). Similar results were confirmed in a biodistribution study of FITC-TrapG and NIR-TrapG (Figure S1 in the Supporting Information). However, some nonspecific signals were detected in the liver, kidney, bladder, and intestines. This result suggests that the glucuronide trapping probe was eliminated by both the urinary and hepatobiliary routes. We conclude that the glucuronide trapping probes can image βG activity in live animals.

Imaging of βG Activity in Tumors Transplanted in Livers. Deep tissues present a major technical challenge to optical imaging. To test whether NIR-TrapG can be used for deep-tissue imaging, we injected NIR-TrapG to BALB/c nude mice that had CT26 or CT26/mβG tumors transplanted under their liver capsules. FITC-TrapG was also injected in separate mice with liver tumors. Figure 6A shows that NIR signals were detected in live mice bearing CT26/mβG tumors in their livers. Consistent with the noninvasive imaging results, significantly stronger NIR signals were recorded in livers isolated from mice bearing CT26/mβG tumor transplants than in mice bearing control CT26 tumors. On the contrary, no FITC signal was detected in live mice; FITC signals were only detected when animals were killed and livers were placed directly under the detector (Figure 6B). Collectively, these results demonstrate that NIR-TrapG can detect βG activity in deep tissues.

DISCUSSION

We have developed an NIR glucuronide trapping probe (NIR-TrapG) for in vivo imaging of βG expression in deep tissues. βG-mediated hydrolysis of the glucuronyl bond of NIR-TrapG leads to cross-linking of the probe onto nearby nucleophiles at βG-expressing sites. The in vitro analyses demonstrated that this novel glucuronide trapping probe does not affect βG activity and that the activated probe can label bystander proteins. The high penetrability of NIR signals through tissues renders this probe especially useful for noninvasive optical imaging of βG expression in deep tissues.

NIR-fluorescent dyes are useful for biomedical studies. NIR fluorochromes (λ_{em} = 700−900 nm) have high signal/background ratios and penetrate tissues better than those with shorter wavelengths.[23−25] A β-galactosidase (LacZ)-activated far-red probe (DDOAG, λ_{em} = 659 nm) that facilitates noninvasive monitoring of the expression and activity of LacZ in vivo has been reported.[26] Moreover, a PEGylated NIR probe (PEG-NIR797, λ_{em} = 797 nm) can detect lung metastasis in vivo.[27] Adams and colleagues also reported that epidermal growth factor (EGF) conjugated with an NIR dye (λ_{em} = 800 nm) produced better images of EGF-receptor-positive tumors than Cy5.5 (λ_{em} = 710 nm).[28] In this report, we have demonstrated that NIR-TrapG (λ_{em} = 820 nm), but not FITC-TrapG, can be used to visualize βG-expressing tumors in deep tissues (liver).

Activity-based probes have gained marked success for in vivo profiling of enzymatic activities, including proteases,[25,29] thymidine kinases,[30,31] and galactosidases.[26,32] This concept

dx.doi.org/10.1021/ja209335z | J. Am. Chem. Soc. 2012, 134, 3103−3110

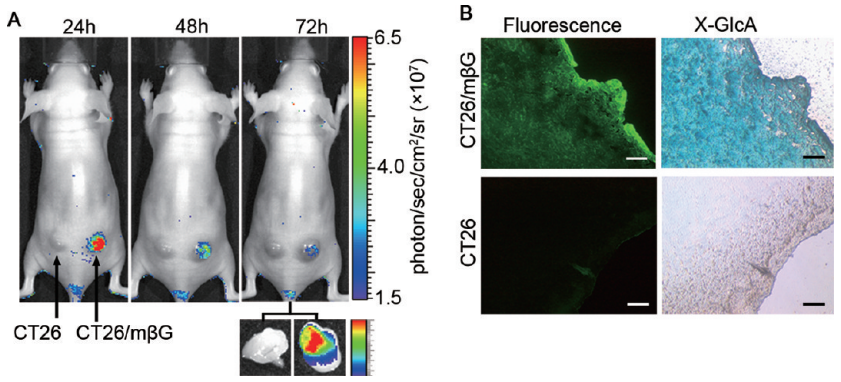

Figure 4. Specific activation of FITC-TrapG in vivo. FITC-TrapG was intravenously injected into BALB/c nude mice bearing CT26/mβG (right flank) and CT26 (left flank) tumors. (A) In vivo optical imaging of FITC-TrapG at 24, 48, and 72 h after probe injection. Tumor tissue was also harvested to confirm specific fluorescent signals. (B) CT26/mβG and CT26 tumors were resected at 24 h after FITC-TrapG injection, stained with X-GlcA, and examined under bright-field and fluorescent field illumination. Scale bar: 100 μm.

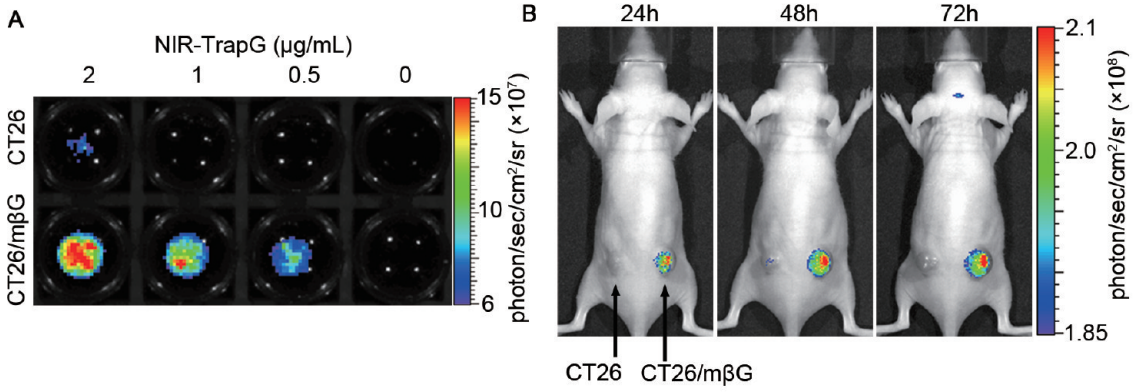

Figure 5. Optical imaging using NIR-TrapG. (A) Optical imaging of CT26/mβG or CT26 cells (3×10^6/well) pretreated with 2, 1, 0.5, or 0 μg/mL of NIR-TrapG. (B) Optical imaging of subcutaneous CT26/mβG and CT26 tumors in mice at 24, 48, and 72 h after probe injection.

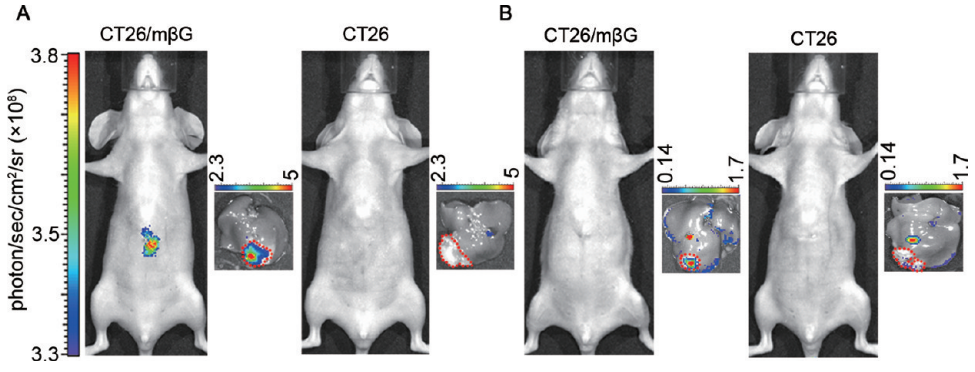

Figure 6. Deep tissue imaging of βG-expressing tumors using NIR-TrapG. NIR-TrapG or FITC-TrapG was injected into BALB/c mice bearing CT26 or CT26/mβG tumor transplants in their livers. Noninvasive optical imaging of (A) NIR-TrapG or (B) FITC-TrapG was performed at 24 h after probe injection. Livers were harvested to confirm the location of the tumors and the specificity of the fluorescent signal. Red dotted lines indicate tumor locations in the liver.

depends heavily on the specific binding of the probe to the active site of the target enzyme. Activity-based probes can irreversibly inactivate the targeted enzymes, as observed for cysteine protease,[33,34] cytosolic 2 class I aldehyde dehydrogenase (cALDH-I),[35] transcriptional activator (LasR),[36] and cytochrome P450.[37] In contrast, enzymatic activation of noninhibitory probes leads to signal amplification and thus improves detection.[33] In addition, noninhibitory imaging probes do not interfere with therapeutic efficiency of enzyme-based prodrug therapies.[25,38] Difluoromethylphenol substrates have been demonstrated to display trapping activity after activation by galactosidases[39] and sialidases[40] but do not irreversibly inactivate enzymes.[41] Our glucuronide trapping probe does not appear to inhibit the βG activity, which would allow enhanced activation of the substrate and therefore improved imaging. Because many glucuronide antitumor prodrugs have been developed, including 9-aminocamptothecin glucuronide (9ACG)[42] and *p*-hydroxyaniline mustard glucur-

dx.doi.org/10.1021/ja209335z | J. Am. Chem. Soc. 2012, 134, 3103−3110

Scheme 1. Chemical Structure and Synthesis of Methyl 1-*O*-(2-Difluoromethyl-4-aminophenyl)-*β*-D-glucopyranuronate (7)

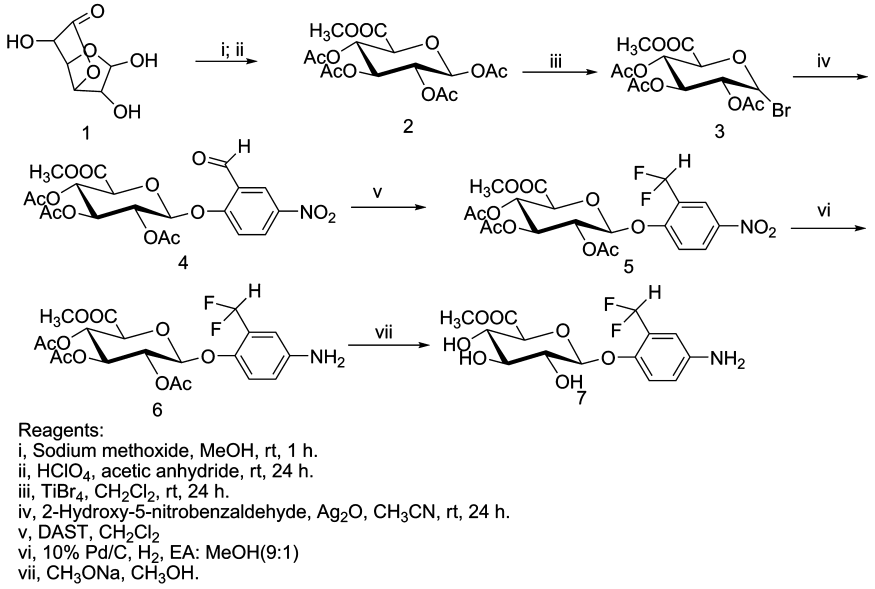

Scheme 2. Formation and Autodegradation of *N*′-Fluorescein-*N*″-[4-*O*-(methyl 2,3,4-tri-*O*-acetyl-*β*-D-glucopyranuronate)-3-difluoromethylphenyl]thiourea (8)

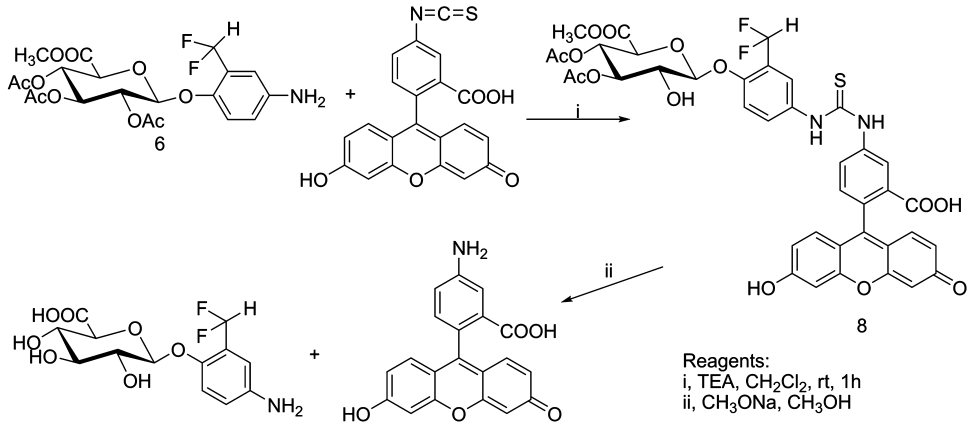

onide (BHAMG),[43] to treat selectively cancers with *β*G overexpression,[4,42] the glucuronide trapping probes may be useful for (1) screening tumors with *β*G overexpression and (2) monitoring the efficacy of glucuronide prodrugs in personalized anticancer therapy.

The trapping moiety (difluoromethylphenol) may be a versatile linker for multiple imaging systems because, at least conceptually, difluoromethylphenol could be coupled to other imaging probes to detect *β*G activity. In this report, we have demonstrated that difluoromethylphenol can be conjugated to two fluorescent probes (FITC and IR-820) for optical imaging. Following derivative chemical principles, difluoromethylphenol could be linked to a glucuronide group with different imaging agents, such as 1,4,7-tricarboxymethylene-1,4,7,10-tetraazacyclododecane (DO3A)[44] and 1,4,7,10-tetraazacyclododecane-*N*,*N*′,*N*″,*N*‴-tetraacetic acid (DOTA)[25] for magnetic resonance imaging or radioiodinated tyramine[4] and fluoroethylamine[45] for nuclear imaging [positron emission tomography (PET) and single-photon emission computed tomography (SPECT)]. The development of *β*G-specific probes may further broaden the selection of tools for monitoring *β*G expression in vivo. Furthermore, the trapping strategy may hold great potential for developing a variety of novel imaging probes to detect other enzymes relevant to human diseases.

■ CONCLUSIONS

The NIR glucuronide trapping probe possesses several attractive attributes. The probe has high penetrability for noninvasive imaging of *β*G activity in deep tissues. The trapping moiety (difluoromethylphenol) does not inhibit *β*G activity, allowing enhancement of the image intensity. On the basis of these advantages, we believe that the glucuronide trapping probe may be a valuable tool for imaging *β*G activity in preclinical studies. The trapping strategy may be extended to other imaging systems or other enzymes.

■ EXPERIMENTAL SECTION

Design and Synthesis of FITC-TrapG and NIR-TrapG. The detailed chemistry procedures are described in the Supporting Information. To develop novel glucuronide trapping probes, FITC and IR-820 were linked to a glucuronide group by a trapping moiety, difluoromethylphenol, to form the activity-based probes FITC-TrapG and NIR-TrapG, respectively. FITC-TrapG and NIR-TrapG were prepared from methyl 1-*α*-bromo-1-deoxy-2,3,4-tri-*O*-acetyl-*β*-D-glu-

dx.doi.org/10.1021/ja209335z | J. Am. Chem. Soc. 2012, 134, 3103−3110

Scheme 3. Chemical Structure and Synthesis of *N′*-Fluorescein-*N″*-[4-*O*-(*β*-D-glucopyranuronic acid)-3-difluoromethylphenyl]-*S*-methylthiourea (FITC-TrapG, 10)

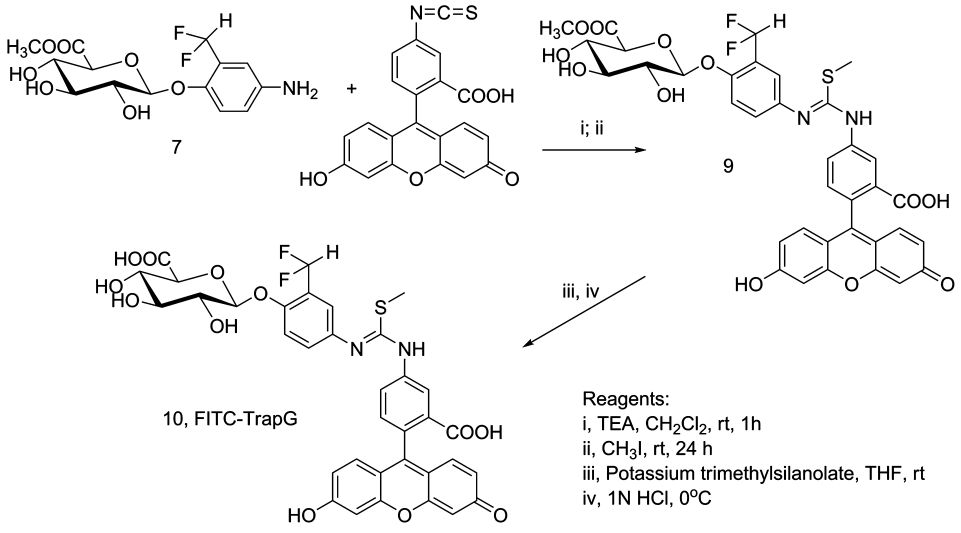

Scheme 4. Chemical Structure and Synthesis of IR-820-Containing Isothiocyanate 13

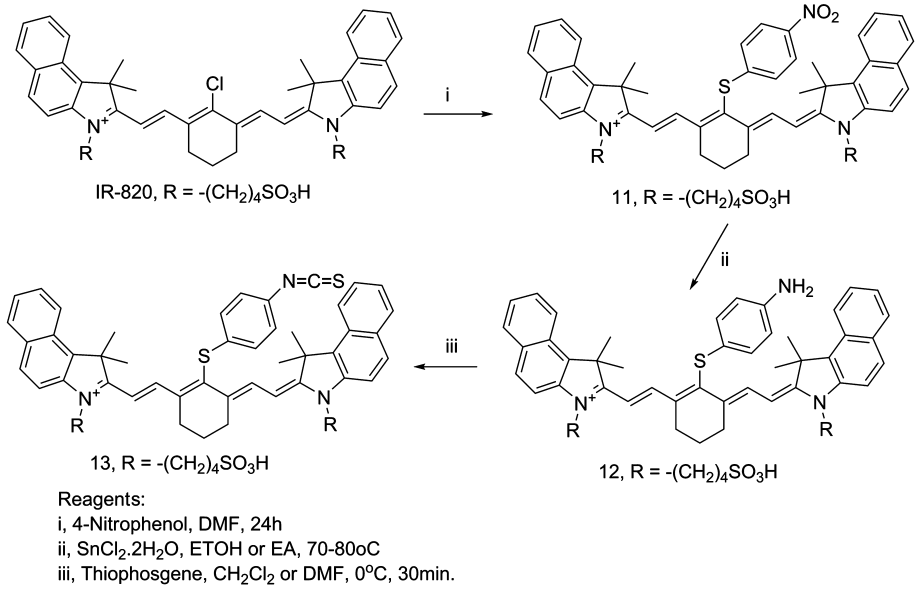

copyranuronate (**3**) and 2-hydroxy-5-nitrobenzaldehyde using a previously published method for the synthesis of glucuronide derivatives[46] with minor modifications. The aldehyde group in **4** was fluorinated to a difluoromethyl group with diethylaminosulfur trifluoride (DAST). The nitro group in **5** was reduced in a palladium-catalyzed reaction to obtain **6** (Scheme 1). For the synthesis of FITC-TrapG, the aniline in **6** was reacted with FITC to obtain methyl *O*-acetyl-protected FITC-TrapG (**8**) (Scheme 2). However, when compound **8** was deprotected with sodium methoxide, the thiourea linkage was hydrolyzed, indicating that the thiourea linkage is susceptible to hydrolysis at basic or physiological pH. Thus, we modified the synthesis pathway to enhance the stability. The acetyl group in compound **6** was deprotected by sodium methoxide to give **7** (Scheme 1). The aniline in **7** was condensed with FITC, after which methyl iodide (CH_3I) was used to create an *S*-methyl pseudothiourea linkage,[47] affording methyl-protected FITC-TrapG (**9**) (Scheme 3). Next, **9** was deprotected with potassium trimethylsilanolate, after which acidification with 1 N HCl afforded FITC-TrapG (**10**).

For the synthesis of NIR-TrapG, the fluorescein group in FITC-TrapG was replaced by an NIR dye (IR-820). The commercial IR-820 chlorocyanine dye was condensed with *p*-nitrothiophenol by nucleophilic substitution to obtain compound **11** (Scheme 4). The nitro group in **11** was reduced using $SnCl_2{\cdot}2H_2O$ to generate an aminothioether dye, compound **12**. The amino group in **12** was reacted with thiophosgene to generate the isothiocyanate, compound **13**. NIR-TrapG was then prepared by the reaction of **7** with **13** followed by addition of CH_3I to create the *S*-methyl pseudothiourea linkage of methyl-protected NIR-TrapG (**14**) (Scheme 5). Next, compound **14** was deprotected with potassium trimethylsilanolate, after which acidification with 1 N HCl afforded NIR-TrapG (**15**).

Cells and Mice. CT26 and CT26/m*β*G cells[9] were maintained in Dulbecco's minimal essential medium (DMEM) (Sigma-Aldrich, St Louis, MO) supplemented with 10% bovine calf serum, 100 *μ*g/mL penicillin, and 100 *μ*g/mL streptomycin at 37 °C in an atmosphere of 5% CO_2. Female BALB/c nude mice (BALB/cAnN.Cg-Foxn1nu/CrlNarl), 5–6 weeks old, were purchased from the National Laboratory Animal Center, Taiwan. The animal experiments were conducted in accordance with the standards set forth by the Kaohsiung Medical University Institutional Animal Care and Use Committee.

dx.doi.org/10.1021/ja209335z | *J. Am. Chem. Soc.* 2012, 134, 3103–3110

Scheme 5. Chemical Structure and Synthesis of the *N*′-(*p*-Aminophenyl)thioether of IR-820-*N*″-[4-*O*-(β-D-Glucopyranuronic acid)-3-difluoromethylphenyl]-*S*-methylthiourea (NIR-TrapG, 15)

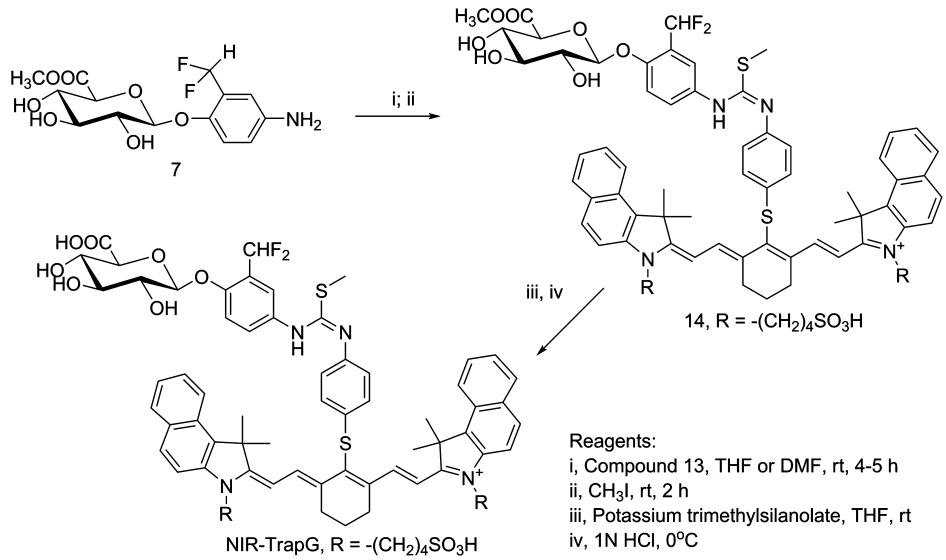

Specific Activation of FITC-TrapG in Vitro. Purified eβG (5 μg/well) and BSA (5 μg/well) (Sigma-Aldrich) were coated overnight in 96-well microtiter plates in phosphate-buffered saline (PBS) (pH 8.0) and then blocked with 5% skim milk at room temperature for 2 h. CT26/mβG and control CT26 cells were seeded at 1.5×10^5 cells/well in 96-well microtiter plates in culture medium overnight. FITC-TrapG was 2-fold serially diluted (starting from 40 μg/mL) in PBS and then added to the proteins or cells at 37 °C for 1 h. The plates were washed with PBS and then stained with a mouse anti-FITC antibody (Sigma-Aldrich) followed by a horseradish peroxidase-conjugated goat anti-mouse immunoglobulin G (IgG) antibody (Jackson ImmunoResearch Laboratories, West Grove, PA). Following three washes with PBS, 2,2′-azinobis(3-ethylbenzothiazoline-6-sulfonic acid) (ABTS) (Sigma-Aldrich) with 0.03% H_2O_2 (Sigma-Aldrich) was added to the wells, and color development was measured on a microplate reader (Molecular Devices, Menlo Park, CA) at OD 405 nm.

βG Enzymatic Activity after FITC-TrapG Treatment. To test whether activated FITC-TrapG inactivates βG enzyme activity, plate-bound 5 μg/well eβG or 1.5×10^5 cells/well CT26/mβG cells were incubated with 40−0 μg/mL FITC-TrapG (2-fold serially diluted) as described above. Following proper washing in PBS, 5 mM *p*-NPG (Sigma-Aldrich) was added to the plates. Color development was measured on a microplate reader at OD 405 nm.

Bystander Trapping of FITC-TrapG. Purified eβG, BSA, or a mixture of eβG/BSA (50 μg) was incubated with FITC-TrapG (40 μg/mL) at 37 °C for 1 h. Proteins were precipitated using cold acetone, centrifuged at 12000*g* for 15 min, electrophoresed on a 10% reducing SDS-PAGE (0.5 μg/lane), and transferred to a nitrocellulose membrane (Pall, Port Washington, NY). Membranes were blocked with 5% skim milk in PBS. FITC attached to proteins was detected by immunoblotting using a mouse anti-FITC antibody (Sigma-Aldrich), a horseradish peroxidase-conjugated goat anti-mouse IgG antibody (Jackson ImmunoResearch Laboratories), and an enhanced chemiluminescence kit (Millipore, Billerica, MA).

In Vivo Imaging of FITC-TrapG and NIR-TrapG. BALB/c nude mice ($n = 3$) bearing CT26 (in left flanks) and CT26/mβG (in right flanks) tumors (50−100 mm^3) were intravenously injected with 500 μg of FITC-TrapG/mouse or 100 μg of NIR-TrapG/mouse in 100 μL of PBS. The fluorescence intensity in the tumors and other internal organs was recorded on an IVIS 50 optical imaging system (Caliper Life Sciences, Hopkinton, MA) at 24, 48, and 72 h after probe injection. We also tested 100 μg of FITC-TrapG/mouse, but there was no significant difference (data not shown). The $\lambda_{ex}/\lambda_{em}$ were 490 nm/525 nm and 710 nm/835 nm for FITC-TrapG and NIR-TrapG, respectively. The acquisition time was 10 s for both probes. We calculated the ratio of fluorescence intensities for the βG-expressing and control tumors as (CT26/mβG − background)/(CT26 − background).

In Vitro Imaging of NIR-TrapG. CT26 and CT26/mβG cells (3×10^6) were stained with 2, 1, 0.5, or 0 μg of NIR-TrapG/mL in PBS containing 0.05% BSA at 37 °C for 2 h. The cells were washed with PBS three times, and the fluorescence was detected on an IVIS 50 optical imaging system.

Histological Analysis. Tumors were excised at 24 h after FITC-TrapG injection, embedded in OCT compound (Tissue-Tek, Torrance, CA) at −80 °C, and sectioned into 10 μm slices. Adjacent tumor sections were stained for βG activity with the β-glucuronidase Reporter Gene Staining Kit (Sigma-Aldrich). The sections were viewed in bright-field and fluorescence modes on an Eclipse TE2000-U inverted microscope (Nikon, Tokyo, Japan).

Tumor Transplantation into Liver and Tumoral Imaging Using FITC-TrapG or NIR-TrapG. After BALB/c nude mice were anesthetized with ketamine/xylazine (135 mg/kg; 15 mg/kg), the abdomenal cavities were surgically opened, and 0.1 cm × 0.2 cm pieces of CT26/βG or CT26 tumors were transplanted under the capsule of the livers ($n = 3$ for each group). One week after the transplantation, mice were intravenously injected with 500 μg of FITC-TrapG/mouse or 100 μg of NIR-TrapG/mouse in 100 μL of PBS. Whole-body fluorescent signals were recorded on an IVIS 50 optical imaging system at 24 h after probe injection. After noninvasive imaging, the livers were harvested and placed directly under the detector of the IVIS 50 system to reaffirm the location of the tumors.

■ ASSOCIATED CONTENT

Ⓢ Supporting Information

Detailed chemistry procedures, NMR data, and biodistribution of FITC-TrapG and NIR-TrapG. This material is available free of charge via the Internet at http://pubs.acs.org.

■ AUTHOR INFORMATION

Corresponding Author

tlcheng@kmu.edu.tw.; yulin@mail.chna.edu.tw

Author Contributions

◆These authors contributed equally.

■ ACKNOWLEDGMENTS

This work was supported by grants from the National Research Program for Biopharmaceuticals, National Science Council, Taipei, Taiwan (NSC 100-2325-B-037-001, 100-2320-B-041-002, NSC98-2320-B-041-003), Academia Sinica (AS-98-TP-B09), the Department of Health, Executive Yuan, Taiwan (DOH100-TD-N-111-010, DOH100-TD-C-111-002), and Kaohsiung Medical University Research Foundation (KMUER014).

■ REFERENCES

(1) Bosslet, K.; Straub, R.; Blumrich, M.; Czech, J.; Gerken, M.; Sperker, B.; Kroemer, H. K.; Gesson, J. P.; Koch, M.; Monneret, C. *Cancer Res.* **1998**, *58*, 1195.
(2) Juan, T. Y.; Roffler, S. R.; Hou, H. S.; Huang, S. M.; Chen, K. C.; Leu, Y. L.; Prijovich, Z. M.; Yu, C. P.; Wu, C. C.; Sun, G. H.; Cha, T. L. *Clin. Cancer Res.* **2009**, *15*, 4600.
(3) Sperker, B.; Werner, U.; Murdter, T. E.; Tekkaya, C.; Fritz, P.; Wacke, R.; Adam, U.; Gerken, M.; Drewelow, B.; Kroemer, H. K. *Naunyn-Schmiedeberg's Arch. Pharmacol.* **2000**, *362*, 110.
(4) Murdter, T. E.; Friedel, G.; Backman, J. T.; McClellan, M.; Schick, M.; Gerken, M.; Bosslet, K.; Fritz, P.; Toomes, H.; Kroemer, H. K.; Sperker, B. *J. Pharmacol. Exp. Ther.* **2002**, *301*, 223.
(5) de Graaf, M.; Boven, E.; Scheeren, H. W.; Haisma, H. J.; Pinedo, H. M. *Curr. Pharm. Des.* **2002**, *8*, 1391.
(6) Chen, X.; Wu, B.; Wang, P. G. *Curr. Med. Chem. Anticancer Agents* **2003**, *3*, 139.
(7) Jefferson, R. A.; Burgess, S. M.; Hirsh, D. *Proc. Natl. Acad. Sci. U.S.A.* **1986**, *83*, 8447.
(8) Platteeuw, C.; Simons, G.; de Vos, W. M. *Appl. Environ. Microbiol.* **1994**, *60*, 587.
(9) Su, Y. C.; Chuang, K. H.; Wang, Y. M.; Cheng, C. M.; Lin, S. R.; Wang, J. Y.; Hwang, J. J.; Chen, B. M.; Chen, K. C.; Roffler, S.; Cheng, T. L. *Gene Ther.* **2007**, *14*, 565.
(10) Tzou, S. C.; Roffler, S.; Chuang, K. H.; Yeh, H. P.; Kao, C. H.; Su, Y. C.; Cheng, C. M.; Tseng, W. L.; Shiea, J.; Harm, I. H.; Cheng, K. W.; Chen, B. M.; Hwang, J. J.; Cheng, T. L.; Wang, H. E. *Radiology* **2009**, *252*, 754.
(11) Dolbeare, F. A.; Phares, W. *J. Histochem. Cytochem.* **1979**, *27*, 120.
(12) Prosperi, E.; Raap, A. K. *Histochem. J.* **1982**, *14*, 689.
(13) Brot, F. E.; Bell, C. E. Jr.; Sly, W. S. *Biochemistry* **1978**, *17*, 385.
(14) Gallagher, S. R. *GUS Protocols: Using the GUS Gene As a Reporter of Gene Expression*; Academic Press: San Diego, 1992.
(15) Jefferson, R. A. *Nature* **1989**, *342*, 837.
(16) Weissleder, R. *Nat. Biotechnol.* **2001**, *19*, 316.
(17) Ye, Y.; Li, W. P.; Anderson, C. J.; Kao, J.; Nikiforovich, G. V.; Achilefu, S. *J. Am. Chem. Soc.* **2003**, *125*, 7766.
(18) Xing, B.; Khanamiryan, A.; Rao, J. *J. Am. Chem. Soc.* **2005**, *127*, 4158.
(19) Yuan, F.; Verhelst, S. H.; Blum, G.; Coussens, L. M.; Bogyo, M. *J. Am. Chem. Soc.* **2006**, *128*, 5616.
(20) Blum, G.; von Degenfeld, G.; Merchant, M. J.; Blau, H. M.; Bogyo, M. *Nat. Chem. Biol.* **2007**, *3*, 668.
(21) Salisbury, C. M.; Cravatt, B. F. *J. Am. Chem. Soc.* **2008**, *130*, 2184.
(22) Fonovic, M.; Bogyo, M. *Expert Rev. Proteomics* **2008**, *5*, 721.
(23) Kovar, J. L.; Simpson, M. A.; Schutz-Geschwender, A.; Olive, D. M. *Anal. Biochem.* **2007**, *367*, 1.
(24) Ntziachristos, V.; Bremer, C.; Weissleder, R. *Eur. Radiol.* **2003**, *13*, 195.
(25) Mahmood, U.; Weissleder, R. *Mol. Cancer Ther.* **2003**, *2*, 489.
(26) Tung, C. H.; Zeng, Q.; Shah, K.; Kim, D. E.; Schellingerhout, D.; Weissleder, R. *Cancer Res.* **2004**, *64*, 1579.
(27) Chuang, K. H.; Wang, H. E.; Cheng, T. C.; Tzou, S. C.; Tseng, W. L.; Hung, W. C.; Tai, M. H.; Chang, T. K.; Roffler, S. R.; Cheng, T. L. *J. Nucl. Med.* **2010**, *51*, 933.
(28) Adams, K. E.; Ke, S.; Kwon, S.; Liang, F.; Fan, Z.; Lu, Y.; Hirschi, K.; Mawad, M. E.; Barry, M. A.; Sevick-Muraca, E. M. *J. Biomed. Opt.* **2007**, *12*, No. 024017.
(29) Zhu, L.; Xie, J.; Swierczewska, M.; Zhang, F.; Quan, Q.; Ma, Y.; Fang, X.; Kim, K.; Lee, S.; Chen, X. *Theranostics* **2011**, *1*, 18.
(30) Bading, J. R.; Shields, A. F. *J. Nucl. Med.* **2008**, *49* (Suppl. 2), 64S.
(31) Gross, S.; Piwnica-Worms, D. *Cancer Cell* **2005**, *7*, 5.
(32) Kamiya, M.; Kobayashi, H.; Hama, Y.; Koyama, Y.; Bernardo, M.; Nagano, T.; Choyke, P. L.; Urano, Y. *J. Am. Chem. Soc.* **2007**, *129*, 3918.
(33) Blum, G.; Weimer, R. M.; Edgington, L. E.; Adams, W.; Bogyo, M. *PLoS One* **2009**, *4*, No. e6374.
(34) Watzke, A.; Kosec, G.; Kindermann, M.; Jeske, V.; Nestler, H. P.; Turk, V.; Turk, B.; Wendt, K. U. *Angew. Chem., Int. Ed.* **2008**, *47*, 406.
(35) Adam, G. C.; Cravatt, B. F.; Sorensen, E. J. *Chem. Biol.* **2001**, *8*, 81.
(36) Amara, N.; Mashiach, R.; Amar, D.; Krief, P.; Spieser, S. A.; Bottomley, M. J.; Aharoni, A.; Meijler, M. M. *J. Am. Chem. Soc.* **2009**, *131*, 10610.
(37) Wright, A. T.; Song, J. D.; Cravatt, B. F. *J. Am. Chem. Soc.* **2009**, *131*, 10692.
(38) McIntyre, J. O.; Matrisian, L. M. *J. Cell. Biochem.* **2003**, *90*, 1087.
(39) Janda, K. D.; Lo, L. C.; Lo, C. H.; Sim, M. M.; Wang, R.; Wong, C. H.; Lerner, R. A. *Science* **1997**, *275*, 945.
(40) Lu, C. P.; Ren, C. T.; Lai, Y. N.; Wu, S. H.; Wang, W. M.; Chen, J. Y.; Lo, L. C. *Angew. Chem., Int. Ed.* **2005**, *44*, 6888.
(41) Hanson, S. R.; Whalen, L. J.; Wong, C. H. *Bioorg. Med. Chem.* **2006**, *14*, 8386.
(42) Prijovich, Z. M.; Chen, B. M.; Leu, Y. L.; Chern, J. W.; Roffler, S. R. *Br. J. Cancer* **2002**, *86*, 1634.
(43) Wang, S. M.; Chern, J. W.; Yeh, M. Y.; Ng, J. C.; Tung, E.; Roffler, S. R. *Cancer Res.* **1992**, *52*, 4484.
(44) Duimstra, J. A.; Femia, F. J.; Meade, T. J. *J. Am. Chem. Soc.* **2005**, *127*, 12847.
(45) Antunes, I. F.; Haisma, H. J.; Elsinga, P. H.; Dierckx, R. A.; de Vries, E. F. *Bioconjugugate Chem.* **2010**, *21*, 911.
(46) Leu, Y. L.; Roffler, S. R.; Chern, J. W. *J. Med. Chem.* **1999**, *42*, 3623.
(47) Zheng, W.; Papiernik, S. K.; Guo, M.; Yates, S. R. *Environ. Sci. Technol.* **2004**, *38*, 1188.